

Short Communications

Prediction of the pressure drop across a gas-solid semi-fluidized bed

G. K. ROY* and P. SEN GUPTA

Department of Chemical Engineering, Indian Institute of Technology, Kharagpur, W. Bengal (India)

(Received 3 December 1971)

The necessity of having a generalized correlation for the prediction of the pressure drop across a semi-fluidized bed is stressed. Pressure drops across the semi-fluidized bed have been calculated using various theoretical equations and have been compared with the experimental values. For the first time, two different equations, one for spherical particles and the other for non-spherical ones, have been suggested for the prediction of the actual pressure drop in terms of the system variables.

Semi-fluidization is a new and unique type of fluid-solid contact operation, which has only been reported in the last decade. Like packed bed and fluidized bed operations, this is also a two-phase phenomenon. A semi-fluidized bed is a compromise between the packed bed and fluidized bed conditions, in which certain drawbacks of both these operations are eliminated¹. The introduction of a porous disc or sieve in a conventional fluidizer arrests the free upward motion of the particles, resulting in the formation of a semi-fluidized bed—the combination of a packed bed at the top and a fluidized portion at the bottom.

In the field of semi-fluidization, more attention has been paid to the momentum transfer aspects than to other studies. Although some information is available for the prediction of the minimum and maximum semi-fluidization velocities, and also for the prediction of packed bed formation in semi-fluidization, information for finding the pressure drop across the bed is scanty. An attempt has therefore been made to develop correlations for the prediction of the pressure drop across a gas-solid semi-fluidized bed.

Experimental

The experimental set-up used in the present study is

* Present address: Department of Chemical Engineering, Regional Engineering College, Rourkela-8, Orissa, India.

shown in Fig. 1. The semi-fluidizer was a Perspex column 4.5 cm in internal diameter and 57 cm long. The bottom grid was a 150 mesh stainless-steel screen.

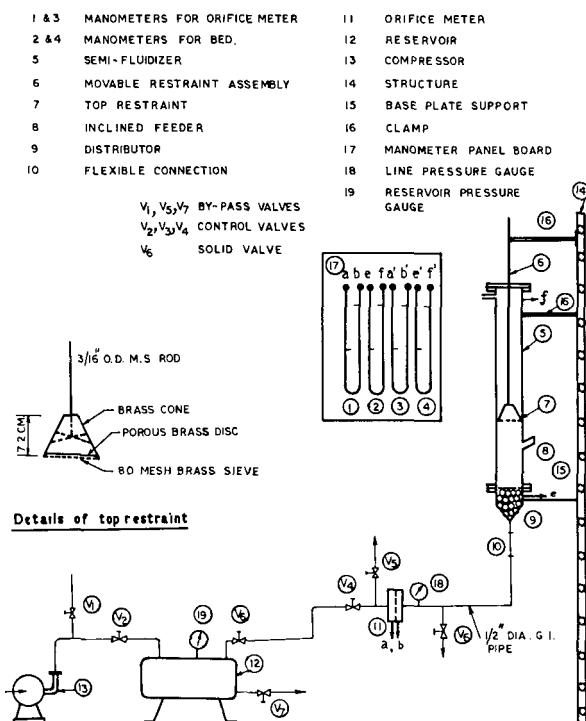


Fig. 1. Schematic diagram of the experimental set-up.

A movable restraint made from a porous brass plate and an 80 mesh brass screen, both soldered to a brass cone, was fixed rigidly to a mild steel rod $\frac{3}{16}$ in. in diameter extending from the top of the semi-fluidizer. Two pressure taps were provided for the orifice meter to record the flow rate of air through the column. The bed pressure drop was noted at two pressure taps, one below the bottom of the grid and the other at the top of the column. Two sets of manometers were provided for the measurement of flow rates and pressure drops, one being used for the lower range and the other for the higher.

While taking a run, the sample was introduced into the column and the fixed bed height was noted. The movable restraint was adjusted for a particular bed expansion ratio. Pressure drops across the bed and the orifice were noted as the air flow rate was increased. When semi-fluidization sets in, the top bed formations

were constantly recorded. The static and expanded bed porosities were determined in separate experiments with samples of known weight. The surface area of the particles and the shape factors were determined by the air permeability method².

Results and discussion

Altogether 141 sets of runs were made. Two spherical materials (mustard seed and sago of size 14/20 BSS) and four non-spherical materials (table salt, sand, magnesite and ammonium sulphate of size 30/40 BSS)

were studied. In addition, for table salt only, four size ranges (20/30, 30/40, 40/52 and 52/60 BSS) were examined. The lowest and highest densities of solids used were 1.12 and 2.80 g/cm³ respectively. The properties of the solid particles and the fluids used are given in detail in Table 1. Table 2 gives a typical run showing the variation of pressure drop and packed bed formation with fluid mass velocity. These effects are shown in Fig. 2. The bed expansion data for the same system are given in Table 3 and illustrated in Fig. 3.

TABLE 1

Physical properties of fluids used

Sl. no.	Fluid	Temperature (°C)	Density (g/cm ³)	Viscosity (poise)	Use
1	Air at 1 atm pressure	22	0.00012	0.00018	Fluidizing medium
2	Carbon tetrachloride	22	1.583	—	Manometer liquid
3	Mercury	22	13.600	—	Manometer liquid

Physical characteristics of materials used

Sl. no.	Materials used	Particle size		Density ρ_s (g/cm ³)	Packed bed porosity ϵ_{pa}	Surface area S_v (cm ² /m ³)	Sphericity ϕ_s
		Mesh no. BSS	d_p (m $\times 10^4$)				
<i>Non-spherical</i>							
1	Table salt	20/30	7.51	2.100	0.596	241.0	0.331
2	Table salt	30/40	4.42	2.100	0.588	300.5	0.452
3	Table salt	40/52	3.38	2.100	0.560	302.0	0.587
4	Table salt	52/60	2.74	2.100	0.533	335.0	0.654
5	Ammonium sulphate	30/40	4.42	1.763	0.377	136.0	1.000
6	Sand	30/40	4.42	2.650	0.451	170.5	0.798
7	Magnesite	30/40	4.42	2.800	0.443	177.0	0.770
<i>Spherical</i>							
8	Mustard seed	14/20	11.05	1.120	0.362	54.2	1.000
9	Sago	14/20	11.05	1.304	0.380	54.2	1.000

TABLE 2

Variation of pressure drop and packed bed formation (below the top restraint) with fluid mass velocity

System: salt-air; particle size: 20/30 BSS; $h_s = 9$ cm; $h = 27$ cm; $R \approx 3.0$; $t = 23^\circ\text{C}$

Sl. no.	ΔH_1 (cm of CCl ₄)	ΔP (kg/m ²)	ΔH_2 (cm of . . .)	G (kg/h m ²)	h_{pa} (cm)	h_{pa}/h_s
1	1.5	23.8	3.9 CCl ₄	741	—	—
2	2.5	39.6	8.8 CCl ₄	1125	—	—
3	3.5	55.5	14.7 CCl ₄	1453	—	—
4	3.9	61.8	16.6 CCl ₄	1547	—	—
5	4.2	66.6	28.8 CCl ₄	2045	—	—
6	4.4	69.8	34.9 CCl ₄	2250	—	—
7	4.6	73.0	6.3 Hg	2840	—	—
8	6.4	101.5	8.9 Hg	3365	—	—
9	9.1	144.2	12.2 Hg	3950	1.5	0.166
10	17.2	272.5	24.3 Hg	5590	3.0	0.333
11	25.6	405.5	33.8 Hg	6585	4.0	0.444
12	40.6	644.0	45.1 Hg	7600	5.0	0.555

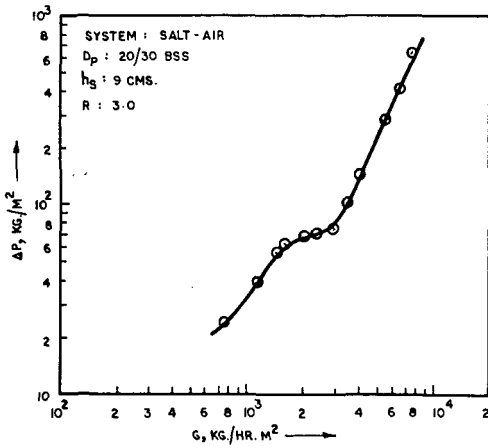


Fig. 2. Variation of pressure drop with fluid mass velocity.

TABLE 3

Variation of expanded bed height and bed porosity with fluid mass velocity

System: salt - air; particle size 20/30 BSS; $w = 64.6597$ g; $h_s = 4.8$ cm; $v_s = 30.8$ cm³; $\epsilon_{pa} = 0.596$, $t = 19^\circ\text{C}$

Sl. no.	ΔH_2 (cm of . . .)	G (kg/h m ²)	h_f (cm)	h_f/h_s	ϵ_f
1	14.2 CCl ₄	1420	5.0	1.040	0.612
2	26.4 CCl ₄	1950	5.8	1.210	0.664
3	32.0 CCl ₄	2152	6.2	1.290	0.688
4	37.7 CCl ₄	2340	6.5	1.355	0.702
5	43.1 CCl ₄	2505	6.8	1.417	0.715
6	6.7 Hg	2945	7.8	1.625	0.752
7	8.3 Hg	3270	8.4	1.750	0.770
8	10.0 Hg	3585	9.5	1.980	0.796
9	11.7 Hg	3870	10.1	2.100	0.808
10	13.2 Hg	4110	11.0	2.290	0.824
11	15.9 Hg	4530	11.9	2.480	0.837
12	19.1 Hg	4955	13.0	2.706	0.851
13	23.3 Hg	5470	14.5	3.020	0.866
14	27.3 Hg	5910	16.5	3.440	0.882
15	31.8 Hg	6390	17.3	3.600	0.888
16	38.5 Hg	7030	18.6	3.870	0.896
17	46.9 Hg	7750	22.6	4.700	0.915

Prediction of pressure drop in a semi-fluidized bed. The pressure drop in a semi-fluidized bed should, ideally, be equal to the algebraic sum of the pressure drops across the fluidized section and the packed section, since they are aligned in series in the direction of flow. While there is only one generalized equation³, namely

$$\left(\frac{\Delta P}{L}\right)_f = (\rho_s - \rho_f)(1 - \epsilon_f) \quad (1)$$

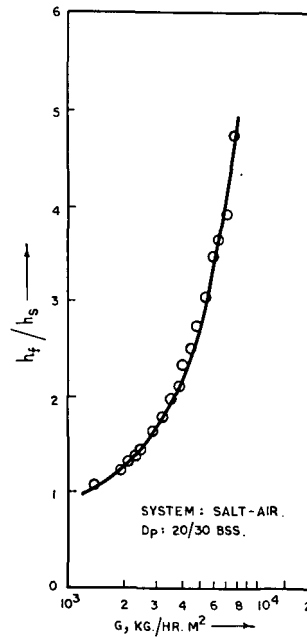


Fig. 3. Variation of expanded bed height with fluid mass velocity.

for the prediction of the pressure drop across a fluidized bed, there are various correlations for the determination of the pressure drop across a packed bed. A few important ones are as follows.

(a) The Kozeny-Carman equation⁴:
for laminar flow ($G/a\mu < 100$)

$$\left(\frac{\Delta P}{L}\right)_{pa} = \frac{5G^2a}{g_c \rho_f \epsilon_{pa}^3} \left(\frac{G}{a\mu}\right)^{1.0} \quad (2a)$$

and for turbulent flow ($G/a\mu \geq 100$)

$$\left(\frac{\Delta P}{L}\right)_{pa} = \frac{0.4 G^2a}{g_c \rho_f \epsilon_{pa}^3} \left(\frac{G}{a\mu}\right)^{0.1} \quad (2b)$$

(b) The equation of Leva³ and coworkers:

$$\left(\frac{\Delta P}{L}\right)_{pa} = \frac{2fG^2}{g_c \rho_f d_p} \frac{1}{\phi_s^{3-n}} \frac{(1 - \epsilon_{pa})^{3-n}}{\epsilon_{pa}^3} \quad (3)$$

where $n = 1$ for laminar flow, $n = 2$ for turbulent flow and f is the modified friction factor. The values of n and f are determined from a knowledge of the state of flow and reference to the standard plot of f versus Re_p ⁴.

(c) Ergun's equation³:

$$\left(\frac{\Delta P}{L}\right)_{pa} = 150 \frac{(1 - \epsilon_{pa})^2}{\epsilon_{pa}^3} \frac{\mu u}{d_p^2} + 1.75 \left(\frac{1 - \epsilon_{pa}}{\epsilon_{pa}^3}\right) \frac{Gu}{d_p} \quad (4)$$

Fan *et al.*⁵ measured the total pressure drop occurring during semi-fluidization and compared these measured values with those calculated from correlations. They used Ergun's equation for calculation of the pressure drop for the packed section. The equation for the total pressure drop was given as

$$\begin{aligned} \Delta P_t &= \left(\frac{\Delta P}{L}\right)_{pa} h_{pa} + \left(\frac{\Delta P}{L}\right)_f (h - h_{pa}) \\ &= \left[150 \left(\frac{1 - \epsilon_{pa}}{\epsilon_{pa}^3}\right) \frac{\mu u}{d_p^2} + 1.75 \left(\frac{1 - \epsilon_{pa}}{\epsilon_{pa}^3}\right) \frac{Gu}{d_p} \right] \times \\ &\quad \times \left[(h_f - h) \frac{1 - \epsilon_f}{\epsilon_f - \epsilon_{pa}} \right] \frac{1}{g_c} + \quad (5) \\ &\quad + \left[h_f - \frac{(1 - \epsilon_{pa})(h_f - h)}{\epsilon_f - \epsilon_{pa}} \right] (1 - \epsilon_f)(\rho_s - \rho_f) \end{aligned}$$

obtained in each case by adding the packed bed pressure drop to the fluidized bed pressure drop obtained from eqn. (1), and these values were then compared with the experimental values (Table 5). It was found that use of the Kozeny—Carman equation gave much lower values in all cases, whereas the equation suggested by Leva gave a few values higher than the experimental ones and the rest lower. The values of pressure drops as calculated by Ergun's equation were found to be on the lower side. In further work Ergun's equation only was used for the calculation of the packed bed pressure drop. The use of Leva's equation, although justified to some extent (because of its closeness to the experimental values in some cases), was not favoured since it involves quantities like the modified friction factor *f* and the state of flow factor *n* which must be taken from charts. It is difficult to read the exact values of these quantities and any error here would manifest itself in the form of wide deviations. In addition, Leva has suggested different equations for the packed bed pressure drop taking into account the effect of surface roughness (a quantity that cannot be measured directly)³. In contrast, Ergun's equation is quite simple as it involves quantities which are directly measurable.

Development of the correlation. As has been reported earlier⁶ and has also been observed in the present case, the porosity of the packed section causes difficulty in the calculation of the over-all pressure drop in the semi-fluidized bed. Available equations for packed bed pressure drops are quite sensitive to bed porosity variations. Also, there is no direct way of simultaneously measuring the porosities of the fixed

TABLE 4
Comparison of packed bed pressure drops

<i>Spherical—system: mustard seed—air; d_p: 0.001105 m</i>				<i>Non-spherical—system: salt—air; d_p: 0.000442 m</i>			
Sl. no.	Pressure drop (kg/m ²)			Sl. no.	Pressure drop (kg/m ²)		
	by Kozeny—Carman eqn.	by Leva's eqn.	by Ergun's eqn.		by Kozeny—Carman eqn.	by Leva's eqn.	by Ergun's eqn.
1	2.12	7.34	6.42	1	1.63	9.35	2.01
2	11.90	22.80	21.40	2	14.75	91.00	21.90
3	35.80	97.40	85.50	3	32.70	208.00	54.50
4	60.30	155.20	135.00	4	36.80	205.50	57.60
5	69.20	159.00	139.20	5	40.50	242.00	55.00
6	146.50	385.00	336.50	6	54.20	350.00	82.90
				7	60.90	360.00	88.00
				8	81.10	517.00	133.50
				9	83.90	568.00	157.50
				10	97.00	618.00	156.30
				11	105.40	719.00	188.60
				12	116.50	783.00	206.00
				13	120.00	793.00	204.00

TABLE 5

Total pressure drop of semi-fluidized bed

Non-spherical particles—system: salt—air; d_p : 0.000442 m

Sl. no.	by Kozeny-Carman eqn.	by Leva's eqn.	by Ergun's eqn.	Experimental
1	84.60	92.30	85.01	169.6
2	91.85	168.10	99.00	242.5
3	97.20	272.50	119.00	323.0
4	97.70	266.40	118.50	347.0
5	94.40	295.90	108.90	250.5
6	106.70	402.50	135.40	330.0
7	103.40	402.50	130.50	323.0
8	119.90	555.80	172.30	461.0
9	131.00	615.10	198.60	531.0
10	126.20	647.20	185.50	555.0
11	144.60	758.20	227.80	548.5
12	147.10	813.60	236.60	645.0
13	144.40	817.40	228.40	670.0

Spherical particles—system: mustard seed—air; d_p : 0.001105 m

1	58.12	73.30	62.40	331.5
2	65.30	76.20	74.80	198.0
3	87.50	149.10	137.20	366.0
4	107.40	202.20	182.00	398.0
5	110.40	200.20	180.40	314.0
6	175.30	413.80	365.30	469.0

and the fluidized sections of the semi-fluidized bed. This results in a wide variation between the experimental and calculated values of the pressure drops in the bed. Hence an attempt has been made in the present work to give a correction factor, in terms of system variables, which can be used for the prediction of the pressure drop in the semi-fluidized bed.

The pressure drop expression can now be written as

$$(\Delta P_t)_{\text{expt}} = C(\Delta P_t)_{\text{cal}} \quad (6)$$

where $(\Delta P_t)_{\text{expt}}$ is the experimental value of the total pressure drop, $(\Delta P_t)_{\text{cal}}$ is the calculated value of the total pressure drop and C is the correction factor. Rearranging, we get

$$\frac{(\Delta P_t)_{\text{expt}}}{(\Delta P_t)_{\text{cal}}} = C \quad (7)$$

It is imperative that the correction factor should be related to the system parameters. The parameters of importance in this case are

$$\frac{D_c}{d_p}, \quad \frac{\rho_s}{\rho_f}, \quad \frac{h_s}{D_c}, \quad R \quad \text{and} \quad \frac{h_{pa}}{h_s}$$

The relation can be written in the following manner:

$$C = \psi \left[\frac{D_c}{d_p}, \quad \frac{\rho_s}{\rho_f}, \quad \frac{h_s}{D_c}, \quad R, \quad \frac{h_{pa}}{h_s} \right] \quad (8)$$

or

$$C = A \left(\frac{D_c}{d_p} \right)^{a_1} \left(\frac{\rho_s}{\rho_f} \right)^{a_2} \left(\frac{h_s}{D_c} \right)^{a_3} (R)^{a_4} \left(\frac{h_{pa}}{h_s} \right)^{a_5} \quad (9)$$

where A is a constant and a^1, a^2, a^3, a^4 and a^5 are exponents of the system variables.

The exponents of eqn. (9) have been evaluated by plotting the correction factor against each of the system variables on log—log paper. After substitution of these exponents, eqn. (9) becomes

$$C = A \left(\frac{D_c}{d_p} \right)^{-0.415} \left(\frac{\rho_s}{\rho_f} \right)^{0.935} \left(\frac{h_s}{D_c} \right)^{-1.614} (R)^{1.23} \times \left(\frac{h_{pa}}{h_s} \right)^{0.504} \quad (10)$$

where A is the coefficient of the over-all product. If B is the exponent of the over-all product (prod.) which is the correlation factor for the exponents of the system variables, the equation

$$C = A (\text{prod.})^B \quad (11)$$

is valid.

The correction factor has been plotted on log—log paper (Fig. 4) against the product

$$\left(\frac{D_c}{d_p} \right)^{-0.415} \left(\frac{\rho_s}{\rho_f} \right)^{0.935} \left(\frac{h_s}{D_c} \right)^{-1.614} (R)^{1.23} \left(\frac{h_{pa}}{h_s} \right)$$

Two different straight lines with slopes of 0.583 and 1.268 were obtained for spherical and non-spherical particles respectively. The data with asterisks represent conditions of simultaneous variation of a number of variables. In all other cases one parameter was changed at a time, the remainder being kept constant. The equations for the two lines can be written as follows.

For non-spherical particles

$$C = \frac{(\Delta P_t)_{\text{actual}}}{(\Delta P_t)_{\text{calc}}} = 1.95 \times 10^{-1} \left[\left(\frac{D_c}{d_p} \right)^{-0.24} \left(\frac{\rho_s}{\rho_f} \right)^{0.55} \left(\frac{h_s}{D_c} \right)^{-0.94} \times (R)^{0.72} \left(\frac{h_{pa}}{h_s} \right)^{0.29} \right] \quad (12)$$

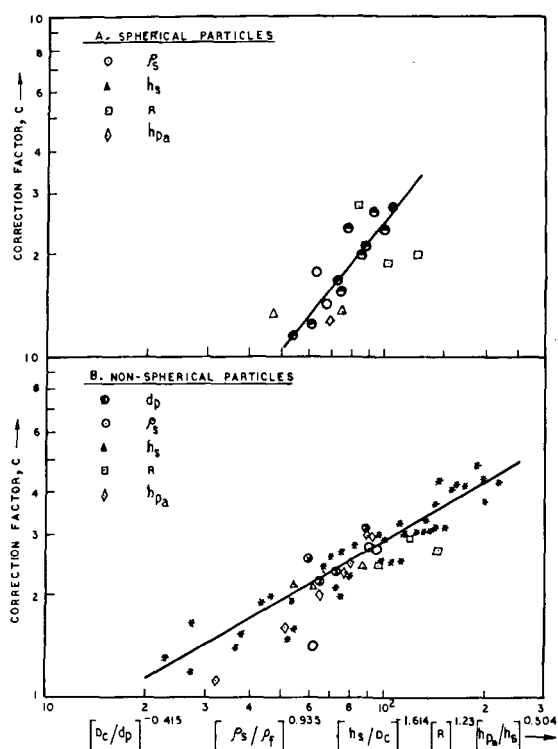


Fig. 4. Relation of C with the system variables.

For spherical particles

$$C = \frac{(\Delta P_t)_{\text{actual}}}{(\Delta P_t)_{\text{calc}}} = 7.3 \times 10^{-3} \left[\left(\frac{D_c}{d_p} \right)^{-0.53} \left(\frac{\rho_s}{\rho_f} \right)^{1.18} \left(\frac{h_s}{D_c} \right)^{-2.05} \times \left(R \right)^{1.56} \left(\frac{h_{pa}}{h_s} \right)^{0.64} \right] \quad (13)$$

The values of the pressure drop calculated by using the above correction factor have been found to be in good agreement with the experimental data. In the case of non-spherical particles, most of the data lie within $\pm 15\%$, the maximum deviation being of the order of 35–40% (for a few cases only). All the system variables have been exhaustively examined. However, the correlation for spherical particles has limitations in that only two materials have been studied. The maximum deviation in this case is as high as 50–60%. It is therefore suggested that further investigations with spherical particles should be carried out.

Nomenclature

- A constant of equation
 a specific surface of the bed, L^2/L^3
 B exponent
 C Pressure drop correction factor
 D_c diameter of column, L
 d_p particle diameter, L
 f modified friction factor
 g_c gravitational constant, $L\theta^{-2}$
 G mass velocity of fluid, $L\theta^{-1}L^{-2}$
 ΔH_1 pressure drop across the bed, L
 ΔH_2 pressure drop across the orifice meter, L
 h over-all height of the column (or semi-fluidized bed), L
 h_s height of the initial static bed, L
 h_{pa} height of the packed section in the semi-fluidized bed, L
 h_f height of the fully fluidized bed, L
 n state of flow factor
 $(\Delta P/L)_f$ pressure gradient across a fluidized bed, FL^{-3}
 $(\Delta P/L)_{pa}$ pressure gradient across a packed bed, FL^{-3}
 ΔP_t over-all pressure drop across the semi-fluidized bed, FL^{-2}
 R bed expansion ratio in semi-fluidization, dimensionless
 S_v surface area of particle per unit volume of solid, L^2/L^3
 u linear velocity of fluid, $L\theta^{-1}$
 w total weight of solid in the column, M
- Greek symbols**
- Δ finite change of variable
 ψ function
 ϕ_s sphericity of particles
 μ viscosity, $ML^{-1}\theta^{-1}$
 ρ density, ML^{-3}
 ϵ bed porosity
- Subscripts**
- c column
f fluid or fluidized bed
pa packed bed
s solid or static bed

References

- 1 L. T. Fan, Y.C. Yang and C. Y. Wen, *A.I.Ch.E. J.*, 5 (1959) 407.
- 2 F. M. Lee and R. W. Nurse, Permeability Method of Fineness Measurement, in *Symp. on Particle Size Analysis*, Inst. Chem. Engrs., London, 1947.
- 3 M. Leva, *Fluidization*, McGraw-Hill, New York, 1959.
- 4 M. S. Walas, *Reaction Kinetics for Chemical Engineers*, McGraw-Hill, New York, 1959.
- 5 L. T. Fan, S. C. Wang and C. Y. Wen, *A.I.Ch.J.*, 9 (1963) 316.
- 6 L. T. Fan and C. Y. Wen, *A.I.Ch.E. J.*, 1 (1961) 606.